Pt/ZrO₂-Al₂O₃ 催化剂催化氧化 C₃H₆ 和 CO 性能

杜君臣 [1,2]　马江丽 [2]　王凤军 [1]　杨冬霞 *,[2,3]　郑婷婷 [1,2]　赵云昆 *,[1]

([1] 昆明贵金属研究所,稀贵金属综合利用新技术国家重点实验室,昆明　650106)

([2] 昆明贵研催化剂有限责任公司,贵金属催化技术与应用国家地方联合工程实验室,昆明　650106)

([3] 昆明理工大学,环境科学与工程学院,昆明　650500)

摘要：采用共沉淀法合成了 ZrO_2 与 Al_2O_3 的不同质量比的 ZrO_2-Al_2O_3 复合氧化物，并以此为载体通过等体积浸渍法制备了 1.5%Pt/ZrO₂-Al₂O₃(w/w)催化剂。以 C₃H₆ 和 CO 为反应物的催化性能评价显示,在系列催化剂中以 Pt/Zr(0.4)-Al 催化剂催化氧化活性最为优异,其 C₃H₆ 和 CO 的起燃温度(T_{50})小于 125 ℃,完全转化温度(T_{90})小于 150 ℃。采用 XRD、低温 N₂ 吸附、H₂-TPR、CO 脉冲吸附等分析表征技术探索了催化剂物相结构、比表面积、颗粒尺寸等对催化活性的影响规律。结果发现,ZrO₂-Al₂O₃ 复合氧化物具有 Al₂O₃ 材料的介孔织构和大比表面积特性,且产生了 $Al_xZr_{1-x}O_y$ 固溶体新物相。适当的 ZrO₂ 与 Al₂O₃ 的质量比,是改善 Pt 与 ZrO₂-Al₂O₃ 的相互作用强度,促进贵金属 Pt 的分散,提升 Pt/ZrO₂-Al₂O₃ 催化剂的低温氧化活性的关键。

关键词：HC&CO 氧化；Pt 基催化剂；ZrO₂-Al₂O₃；尺寸效应；尾气净化

Catalytic Oxidation of C₃H₆ and CO over Pt/ZrO₂-Al₂O₃ Catalyst

DU Jun-Chen[1,2]　MA Jiang-Li[2]　WANG Feng-Jun[1]

YANG Dong-Xia *,[2,3]　ZHENG Ting-Ting[1,2]　ZHAO Yun-Kun *,[1]

([1]*State Key Laboratory of Advanced Technologies for Comprehensive Utilization*

of Platinum Metals, Kunming Institute of Precious Metals, Kunming 650106, China)

([2]*State-Local Joint Engineer Laboratory of Precious Metals Catalytic Technology and*

Application, Kunming Sino-platinum Metals Catalysts Co., Ltd., Kunming 650106, China)

([3]*Faculty of Environmental Science and Engineering, Kunming University of Science and Technology, Kunming 650500, China*)

Abstract: The ZrO₂-Al₂O₃ composite oxides with different mass ratio of ZrO₂ to Al₂O₃ were prepared by co-precipitation method. 1.5%Pt/ZrO₂-Al₂O₃ (w/w) serial catalysts were prepared by isovolume impregnation method. The catalytic performance for C₃H₆ and CO oxidation show that Pt/Zr (0.4)-Al catalyst owns the most excellent catalytic activity. The temperature of light-off (T_{50}) and the complete conversion temperature (T_{90}) were less than 125 and 150 ℃ respectively. The effects of catalyst phase structure, specific surface area and particle size on the catalytic activity were investigated by XRD, N₂ adsorption-desorption, H₂-TPR and CO pulse adsorption. It is found that ZrO₂-Al₂O₃ composite oxides have the mesoporous texture, large specific surface area, and a new phase of $Al_xZr_{1-x}O_y$ solid solution was also produced. The mass ratio of ZrO₂ to Al₂O₃ is the key to improving the interaction between Pt and ZrO₂-Al₂O₃, promoting the dispersion of Pt and enhancing the low temperature oxidation activity of Pt/ZrO₂-Al₂O₃ catalyst.

Keywords: HC&CO oxidation; platinum based catalyst; ZrO₂-Al₂O₃; size effect; exhaust purification

0　Introduction

With the birth of three-way catalyst in 1970s, its contribution to automobile exhaust CO, HC and NO$_x$ purification has been seen widely[1]. In order to improve human′s living environment and meet the stringent environmental regulations, researchers have always been devoted to the improvement of catalyst performance[2-7]. With the implementation of ultra-low and even zero emission regulation, pure single-TWC catalyst is difficult to meet the requirement. It has been agreed that with the installation of close coupled catalyst at engine manifold, the HC and CO emitted during the cold start can be lowered[8].

Due to the large surface area, good adsorption performance, moderate chemical activity and low cost, Al$_2$O$_3$ is widely used as the automobile exhaust gas purification catalyst substrate[9]. However, due to thermal or hydrothermal shock, if the Al$_2$O$_3$ carrier is directly used in the close coupled catalyst, its phase and specific area is liable to change and specific area will decrease rapidly, thus inactivating the catalyst[10]. Researchers have been devoted to improving the thermal stability of Al$_2$O$_3$ since 1940s. The results show that the modification or doping of La, Ce, Pr, Zr, P, Si, Ba, Sr or other elements can delay the high temperature sintering and phase transition of Al$_2$O$_3$ material[11-13]. ZrO$_2$ has the characteristics of acidity, basicity, redox, and is easy to produce oxygen vacancies. However, it also represents the characteristics of small specific surface area and porosity, low mechanical strength, expensive price, and is liable to agglomerate under high temperatures, which will limit its application as the carrier[14]. By understanding the characteristics of Al$_2$O$_3$ and ZrO$_2$, ZrO$_2$-Al$_2$O$_3$ composite oxides with large specific surface area and good heat-resistance were synthesized. When using ZrO$_2$-Al$_2$O$_3$ as carrier, catalyst always shows excellent catalytic activity and selectivity in ethanol reforming, NO reduction, CH$_4$ oxidation and other reactions[15-19].

Studies have showed that Pt and Pd have excellent activity for HC and CO oxidation [20-21]. However, the main work is focusing on the oxidation of HC and CO, Pd and Pd-Rh close coupled catalyst research[22-26], while little focuses on Pt-based catalysts because of the high price in the past. With the continued decline of Pt price in recent years, the study of Pt based oxidation catalysts has shown great significance. In order to obtain high efficiency close coupled catalyst, Pt/Al$_2$O$_3$, Pt/ZrO$_2$-Al$_2$O$_3$ and Pt/ZrO$_2$ serial catalysts were prepared, and characterized by XRD, N$_2$ adsorption-desorption, H$_2$-TPR, CO pulse adsorption and the oxidization system of C$_3$H$_6$ & CO was also studied. The effect of catalyst phase structure, specific surface area and particle size on the catalytic activity of the catalyst were investigated.

1　Experimental

1.1　Materials

All the chemicals were of analytical grade. Pt(NO$_3$)$_2$ solution (62.02 g·L^{-1}) came from Kunming Institute of Precious Metals. ZrO(NO$_3$)$_2$·2H$_2$O, Al(NO$_3$)$_3$ ·2H$_2$O, NH$_3$·H$_2$O (25%) were purchased from Tianjin Guangfu Fine Chemical Research Institute.

1.2　Carrier and catalyst preparation

The ZrO$_2$-Al$_2$O$_3$ composite supports with different mass ratio were prepared by co-precipitation method. NH$_3$·H$_2$O solution was added in the mixed ZrO(NO$_3$)$_2$ solution (0.5 mol·L^{-1}) and Al(NO$_3$)$_3$ solution (0.5 mol·L^{-1}) at room temperature until pH=9, then the obtained precipitate was vigorously stirred for 4 h before being stayed overnight. After being washed several times with distilled water, the mixed sol was dried at 100 ℃ for 12 h, and then calcined at 750 ℃ for 4 h in air. Pure Al$_2$O$_3$ and ZrO$_2$ supports were also prepared in a similar method. The ZrO$_2$(x)-Al$_2$O$_3$ (where mass fraction of ZrO$_2$, x=0, 0.2, 0.4, 0.6, 0.8 and 1) composite was denoted as Zr(x)-Al. The six supports were treated with an aqueous solution of Pt(NO$_3$)$_2$ to obtain a 1.5% (w/w) loading of Pt by an isovolume impregnation. After being dried and calcined at 550 ℃ for 4 h in air, serial catalysts were marked as Pt/Al, Pt/Zr(0.2)-Al, Pt/Zr(0.4)-Al, Pt/Zr(0.6)-Al, Pt/Zr(0.8)-Al, Pt/Zr.

1.2　Catalytic evaluation

The catalytic properties were evaluated using a continuous flow fixed-bed reactor. The catalysts were

sieved through a 40-mesh and a 60-mesh sieve before testing. 0.3 g of the catalyst was evaluated in $1\%CO+0.3\%C_3H_6+5\%O_2+93.7\%N_2$ (V/V) with a space velocity of 18 000 $mL \cdot h^{-1} \cdot g^{-1}$. The purified exhausts were dehydrated by desiccant magnesium chloride first and then measured in Agilent 7890A on-line gas chromatography analyzer. The products were detected by TCD and FID in the analyzer.

1.3 Characterization of catalyst

The X-ray powder diffraction patterns of the catalysts were characterized by Rigaku D/max 2000 powder diffractometer, which was operated at 40 kV and 100 mA using Cu $K\alpha$ (λ=0.154 06 nm) radiation. Inten-sities of the diffraction peaks were recorded in the 2θ range of $10°\sim90°$ with a step size of 0.02°, and the scanning speed was $10° \cdot min^{-1}$.

The N_2 adsoption-desorption was carried out at -196 ℃ on Quanachrome NOVA2000e physisioption apparatus. The specific surface area was calculated using BET method, and pore size and volume were determined using BJH model.

H_2-TPR was measured on Quanachrome CHEMBET 3000 chemical adsorption instrument. 100 mg of catalyst was loaded into a U-shaped tube, heated at a rate of 10 ℃ $\cdot min^{-1}$ to 300 ℃, and kept at 300 ℃ for 1 hour with the Ar gas stream (flow rate 45 mL $\cdot min^{-1}$), and cooled to the ambient temperature afterwards. H_2-TPR was performed in 10.2% (V/V) H_2/Ar mixture gas (flow rate 75 mL $\cdot min^{-1}$) with increasing temperature up to 800 ℃ at a rate of 10 ℃ $\cdot min^{-1}$. The H_2 consumption was measured with a TCD detector.

CO in-$situ$ diffuse reflectance infrared flourier transform spectroscopy (DRIFT) was performed on a near-infrared FT-IR spectrometer manufactured by Themo Nicolet. The spectra were scanned 32 times at a resolution of 4 cm^{-1}. Before the adsorption test, catalyst was reduced, followed by N_2 purging of the pipeline and background signal collection. Afterwards, pure CO gas was introduced for adsorption until a saturated status was reached, then feed gas was switched to N_2 to purge tube residual and signal attributed to CO chemisorbed on the catalyst was recorded.

The dispersion of Pt over the catalyst was determined by CO pulsed adsorption method with CHEMBET 3000 chemical adsorption instrument. The sample was first reduced at 450 ℃ with H_2/He for 2 h at a gas flow rate of 45 mL $\cdot min^{-1}$. And then the feed gas was switched to pure He gas to purge the residual H_2 on the surface or absorbed. When the reaction furnace temperature was cooled to 80 ℃, temperature was kept constant for 30 min. After pulse injecting the high purity CO, CO adsorption signals were recorded with a TCD until no change could be observed in the adsorption peaks. The metal dispersion was calculated by assuming a CO to surface metal atom ratio of 1:1.

2 Results and discussion

2.1 Catalytic activity evaluation

Fig.1 shows the curves of C_3H_6 and CO conversion over Pt/Al_2O_3, Pt/ZrO_2-Al_2O_3, Pt/ZrO_2 serial catalysts under different temperatures. Table 1 lists the C_3H_6 and CO temperature of light-off (T_{50}) and the complete conversion temperature (T_{90}) over a series of catalysts. It can be seen from Table 1 that the T_{50} and
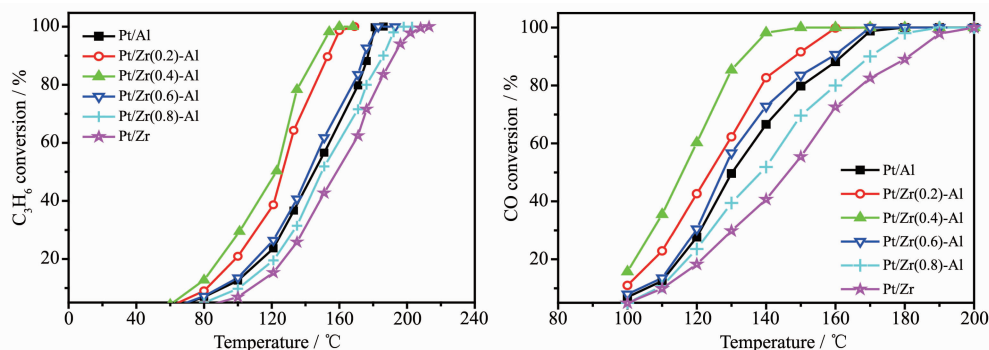

Fig.1　C_3H_6 & CO catalytic oxidation properties over Pt/Al_2O_3, Pt/ZrO_2-Al_2O_3 and Pt/ZrO_2 serial catalysts

Table 1　T_{50} and T_{90} statistics of Pt/Al₂O₃, Pt/ZrO₂-Al₂O₃ and Pt/ZrO₂ serial catalysts

Sample	T_{50} / ℃		T_{90} / ℃	
	C_3H_6	CO	C_3H_6	CO
Pt/Al	145	131	177	162
Pt/Zr(0.2)-Al	126	123	153	148
Pt/Zr(0.4)-Al	122	115	146	134
Pt/Zr(0.6)-Al	142	128	174	159
Pt/Zr(0.8)-Al	149	138	185	170
Pt/Zr	157	147	193	192

T_{90} of the serial catalysts are in the order of Pt/Zr(0.4)-Al<Pt/Zr(0.2)-Al<Pt/Zr(0.6)-Al<Pt/Al<Pt/Zr(0.8)-Al<Pt/Zr. With an increased percentage of ZrO₂ in the carrier, the catalytic activity demonstrates a trend of increasing first and then decreasing. It can be seen that the mass ratio of ZrO₂ to Al₂O₃ in the carrier has a very important effect on the catalytic oxidation activity of Pt/ZrO₂-Al₂O₃ catalyst.

2.2　XRD analysis

In order to understand the effect of the mass ratio of ZrO₂ to Al₂O₃ on the phase structure of the catalyst, serial catalysts were characterized by XRD. The characterization patterns in Fig.2 exhibit that Pt/Al₂O₃ catalyst shows characteristic diffraction peaks at 2θ of 37.4°, 46.0° and 66.7°, which can be attributed to the characteristic diffraction peak of γ-Al₂O₃[27]. For the Pt/ZrO₂-Al₂O₃ catalyst with an increased mass percentage of ZrO₂ in the carrier, the characteristic diffraction peaks of γ-Al₂O₃ gradually diffuse, and the characteristic diffraction peaks of Al$_x$Zr$_{1-x}$O$_y$ solid solu-

tion near 2θ of 30.5°, 35.1°, 50.5° and 60.5° gradually increase[28]. Pt/ZrO₂ catalyst exhibits the characteristic diffraction peaks of monoclinic and tetragonal ZrO₂ near 2θ of 24.1°, 28.2°, 31.5° and 2θ of 30.3°, 35.0°, 50.3°, 60.2°, respectively[29]. However, Pt/Al₂O₃, Pt/ZrO₂-Al₂O₃ and Pt/ZrO₂ serial catalysts haven't showed obvious crystal diffraction peaks of Pt or Pt species, indicating that Pt is highly dispersed in the series of catalysts.

2.3　N₂ adsorption-desorption tests

In order to investigate the effect of ZrO₂ to Al₂O₃ mass ratio on the pore structure and specific surface area of Pt/ZrO₂-Al₂O₃ catalyst, N₂ adsorption-desorption under low temperature was measured over the serial catalysts. The test results are shown in Fig. 3. According to IUPAC classification of adsorption isotherms[30], curves on Pt/Al₂O₃ and Pt/ZrO₂-Al₂O₃ catalysts are close to the adsorption isotherms of type Ⅳ, while the Pt/ZrO₂ catalyst shows a type Ⅰ
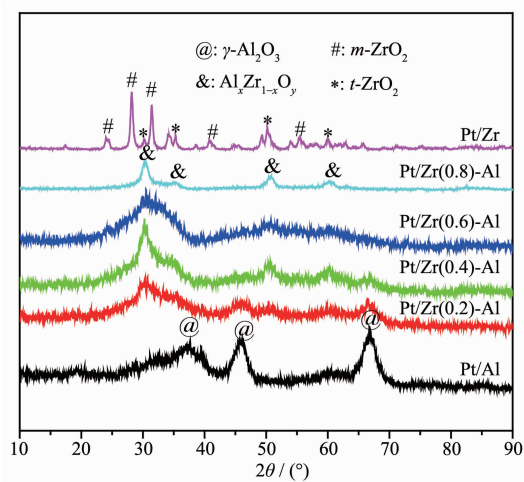

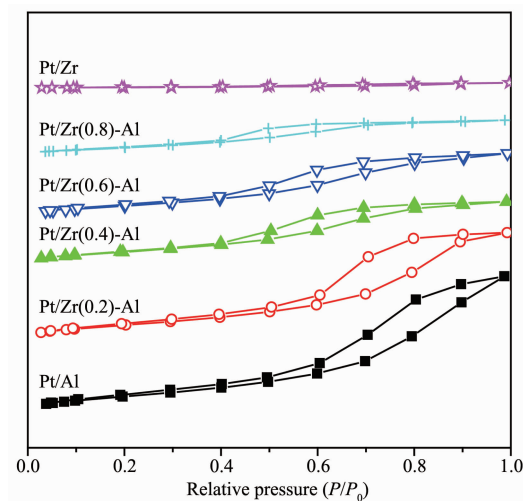Fig.2　XRD patterns of Pt/Al₂O₃, Pt/ZrO₂-Al₂O₃ and Pt/ZrO₂ serial catalysts

Fig.3　N₂ adsorption-desorption isotherm of Pt/Al₂O₃, Pt/ZrO₂-Al₂O₃ and Pt/ZrO₂ serial catalysts

adsorption isotherms. This means that Pt/Al_2O_3 and $Pt/ZrO_2-Al_2O_3$ catalysts own mesoporous textures, while Pt/ZrO_2 catalyst is microporous. Pt/Al_2O_3 and $Pt/ZrO_2-Al_2O_3$ catalysts have a significant H2-type hysteresis loop at P/P_0 of 0.4~1. With increasing of ZrO_2 content in the catalyst carrier, the distance between the upper and lower closing points of the hysteresis loop is getting closer. This indicates that the pore size distribution of the catalyst becomes more and more narrowed with the increase of the mass ratio of ZrO_2 to Al_2O_3 in the carrier[31].

Generally, the large specific surface area catalyst can provide more reactive sites during the catalytic reaction. While the catalyst with large pore volume and size can reduce the diffusion resistance to the mass transfer and improve the catalytic conversion efficiency. It can be seen from Table 2 that the specific surface area, pore volume and pore size of the catalyst show a decreasing trend with increasing mass ratio of ZrO_2 to Al_2O_3 in the carrier. Based on the catalytic activity evaluation data, it is found that the smaller specific surface area, pore volume and pore size may be part of the reasons for a lower catalytic activity of Pt/ZrO_2 and $Pt/Zr(0.8)$-Al.

Table 2　Physical parameters of Pt/Al_2O_3, $Pt/ZrO_2-Al_2O_3$ and Pt/ZrO_2 serial catalysts

Sample	S_{BET} / $(m^2 \cdot g^{-1})$	Pore diameter / nm	Pore volume / $(cm^3 \cdot g^{-1})$	D_{Pt} / nm*
Pt/Al	235	6.2	0.61	3.1
Pt/Zr(0.2)-Al	215	6.0	0.49	2.6
Pt/Zr(0.4)-Al	180	4.5	0.36	2.4
Pt/Zr(0.6)-Al	170	4.4	0.29	2.9
Pt/Zr(0.8)-Al	124	4.0	0.17	4.3
Pt/Zr	6	1.8	0.02	6.4

*Pt particle diameters D_{pt} are estimated from dispersion data[35].

2.4　H₂-TPR analysis

In order to study the effect of the mass ratio of ZrO_2 to Al_2O_3 on the reduction performance of $Pt/ZrO_2-Al_2O_3$ catalyst, the serial catalysts were characterized by H_2-TPR. The characterization patterns are shown in Fig.4. It can be seen that there are roughly two reduction peaks in each catalyst, one at low temperature and another at high temperature, which can be attributed to the reduction of the high dispersion of Pt and the reduction of the large Pt particles, respectively[32]. With increased percentage of ZrO_2 in the carrier, the reduction temperature shifts firstly to lower temperature and then to higher temperature, which is consistent with the evolution of catalytic activity. This indicates that the mass ratio of ZrO_2 to Al_2O_3 in the carrier has an important effect on the interaction strength between Pt and $Al_xZr_{1-x}O_y$ solid solution in $Pt/ZrO_2-Al_2O_3$ catalyst, which affects the catalytic oxidation activity of the catalyst.

Fig.4　H₂-TPR curves of Pt/Al_2O_3, $Pt/ZrO_2-Al_2O_3$ and Pt/ZrO_2 serial catalysts

2.5　Pt particle size analysis

To investigate the effect of ZrO_2 to Al_2O_3 on the Pt particle size in $Pt/ZrO_2-Al_2O_3$ catalyst, the CO *in situ* DRIFTS technique was used. As show in Fig.5, the peaks near 2 050 cm^{-1} correspond to the linear adsorption of CO on the catalyst, while the peaks near 1 835 cm^{-1} correspond to the bridging adsorption of CO on the catalyst[33]. According to previous studies, comparing to the large Pt particle, the Pt atom in each
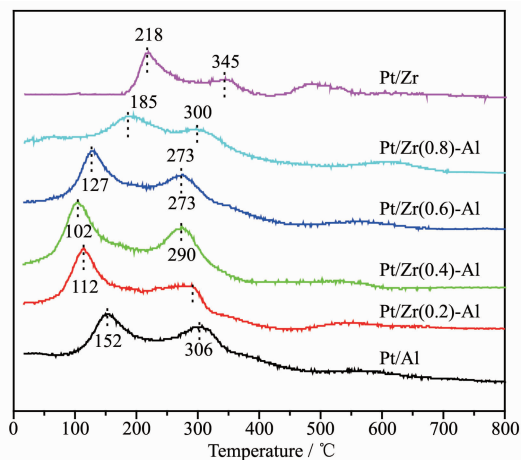
small Pt particle owns less number of Pt-Pt bonds, thus enabling itself to provide more charge density to the $2\pi^*$ orbital of the adsorbed CO. Therefore, the different intensities between linear adsorption and bridge adsorption in the graph correspond to different sizes of Pt particles in the catalyst. The stronger the linear adsorption, the weaker the bridge adsorption, indicating that the Pt particles in the catalyst are smaller and vice versa. It can be seen from Fig.5 that the Pt/ZrO₂-Al₂O₃ catalyst with 40% content of ZrO₂ exhibits the highest ratio of linear adsorption to bridge adsorption intensity, when compared with Pt/Al₂O₃ and Pt/ZrO₂ catalysts, indicating that Pt/Zr(0.4)-Al catalyst owns the smallest Pt particle size in all catalysts.
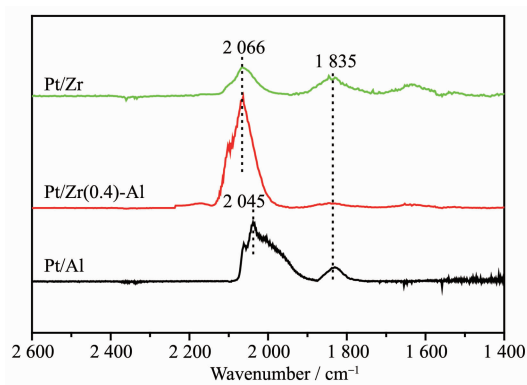

Fig.5　CO *in-situ* DRIFT spectra of Pt/Al₂O₃, Pt/ZrO₂-Al₂O₃ and Pt/ZrO₂ serial catalysts

The Pt particles in Pt/Al₂O₃, Pt/ZrO₂-Al₂O₃ and Pt/ZrO₂ catalysts were quantitatively compared. The results are shown in Table 2 using CO pulse adsorption technique. The results show that the Pt particle size is in the order of Pt/Zr(0.4)-Al<Pt/Zr(0.2)-Al<Pt/Zr(0.6)-Al<Pt/Al<Pt/Zr(0.8)-Al<Pt/Zr. Pt particle size exhibits the trend of decreasing first and then increasing, when the mass percentage of ZrO₂ in the support was increased. This shows that the mass ratio of ZrO₂ to Al₂O₃ is helpful to enhance the interaction between Pt and ZrO₂-Al₂O₃, promote the dispersion of Pt and increase the oxidation activity of Pt/ZrO₂-Al₂O₃ under low temperature, which is consistent with the results of H₂-TPR and catalytic activity.

3　Conclusions

The influence of phase structure, texture properties, reduction properties and particle size on the catalytic oxidation activity of Pt/ZrO₂-Al₂O₃ catalysts were studied. ZrO₂-Al₂O₃ composite oxide carrier shows the mesoporous texture and large specific surface area similar to Al₂O₃, while a new phase of Al$_x$Zr$_{1-x}$O$_y$ solid solution could also be formed, which is beneficial to the dispersion of Pt, reducing the diffusion resistance to mass transfer, as well as improving the catalytic conversion efficiency of catalyst. A suitable mass ratio of ZrO₂ to Al₂O₃ in the carrier is helpful to enhance the interaction between Pt and ZrO₂-Al₂O₃, promote the dispersion of Pt and improve the low temperature oxidation activity of Pt/ZrO₂-Al₂O₃ catalyst. The Pt/ZrO₂-Al₂O₃ catalyst with w_{ZrO_2}:$w_{Al_2O_3}$ = 40:60 exhibits excellent catalytic oxidation activity. The T_{50} and T_{90} of C₃H₆ and CO oxidation is less than 125 and 150 ℃, respectively, demonstrating the material′s potential to be applied in close coupled catalyst.

References:

[1] Morgan C. *Johnson Matthey Technol. Rev.*, **2014**,**58**(4):217-220

[2] Heck R M, Farrauto R J, Weidenkaff A. *Appl. Catal., A*, **2001**,**221**(1):443-457

[3] Gandhi H S, Graham G W, Mccabe R W. *J. Catal.*, **2003**,**216**(1):433-442

[4] KANG Xin-Ting(康新婷), TANG Hui-Ping(汤慧萍), ZHANG Jian(张健), et al. *Rare Metal Materials and Engineering*(稀有金属材料与工程), **2006**,**35**(Suppl.2):442-447

[5] Keav S, Matam S K, Ferri D, et al. *Catalysts*, **2014**,**4**(3):226-255

[6] Wang J H, Chen H, Hu Z C, et al. *Catal. Rev. Sci. Eng.*, **2015**,**57**(1):79-144

[7] Bagwan N, Satpute S. *International Journal of Advanced Production and Industrial Engineering*, **2017**,**504**:22-26

[8] SONG Wei-Cong(宋为聪), SHI Zhong-Hua(史忠华), YAO Yan-Lin(姚艳玲), et al. *Chinese J. Inorg. Chem.*(无机化学学报), **2009**,**25**(5):838-843

[9] Yang C W, Zhang Q, Li J, et al. *J. Energy Chem.*, **2016**,**25**(3):375-380

[10]He J J, Wang C X, Zheng T T, et al. *Johnson Matthey Technol. Rev.*, **2016**,**60**(3):196-203

[11]DU Jun-Chen(杜君臣), CHANG Shi-Ying(常仕英), HUANG Wei-Qiang(黄卫强), et al. *Journal of Molecular Catalysis*

(China)(分子催化), **2015**,**29**(5):482-493

[12]Shen M Q, Song L Y, Wang J, et al. *Catal. Commun.*, **2012**, **22**(18):28-33

[13]Zheng T T, He J J, Xia W Z, et al. *Catal. Commun.*, **2015**, **71**:51-55

[14]LI Ning(李凝), LUO Lai-Tao(罗来涛). *Chin. J. Catal.*(催化学报), **2007**,**28**(9):773-778

[15]Dömök M, Oszkó A, Baán K, et al. *Appl. Catal., A*, **2010**,**383**(1):33-42

[16]Souza M M V M, Aranda D A G, Schmal M. *J. Catal.*, **2001**, **204**(2):498-511

[17]Morán-Pineda M, Castillo S, López T, et al. *Appl. Catal., B*, **1999**,**21**(2):79-88

[18]Long E Y, Wang Y, Zhang X Y, et al. *Chin. J. Catal.*, **2010**, **31**(3):313-316

[19]Wang Y, Tang S Y, Long E, et al. *Chin. J. Catal.*, **2011**,**32**(2):303-308

[20]Cooper J, Beecham J. *Platinum Met. Rev.*, **2013**,**57**(4):281-288

[21]Matsouka V, Konsolakis M, Yentekakis I V, et al. *Top. Catal.*, **2011**,**54**(16/17/18):1124-1134

[22]Shi Z H, Gong M C, Chen Y Q. *Chin. Chem. Lett.*, **2006**,**17**(9):1271-1274

[23]Wang G, Meng M, Zha Y Q, et al. *Fuel*, **2010**,**89**(9):2244-2251

[24]Fang R M, Cui Y J, Chen S J, et al. *Chin. J. Catal.*, **2015**,**36**(2):229-236

[25]Yang X, Yang L Y, Lin S Y, et al. *Chin. J. Catal.*, **2014**,**35**(8):1267-1280

[26]Zhu Z Z, Lu G Z, Guo Y, et al. *J. Ind. Eng. Chem.*, **2012**,**18**(6):2135-2140

[27]DU Jun-Chen(杜君臣), ZHANG Ai-Min(张爱敏), MA Jiang-Li(马江丽), et al. *Chinese J. Inorg. Chem.*(无机化学学报), **2017**,**33**(3):415-420

[28]Wang Y, Xu H D, Shang H Y, et al. *J. Energy Chem.*, **2014**, 23:461-467

[29]Zhao Y J, Zhou J, Zhang J G, et al. *J. Mol. Catal. A*:*Chem.*, **2009**,**309**(1):35-39

[30]Sing K S W. *Pure Appl. Chem.*, **1985**,**57**(4):603-619

[31]XU Hui-Yuan(徐慧远), LUO Jing-Jie(罗靖杰), YAN Chun-Rong(严春蓉), et al. *Journal of Fuel Chemistry and Technology*(燃料化学学报), **2012**,**40**(11):1370-1402

[32]YAN Qian-Gu(严前古), GAO Li-Zhen(高丽珍), YUAN Song-Yue(远松月), et al. *Chem. J. Chinese Universities*(高等学校化学报), **1998**,**19**(8):1300-1303

[33]Bourane A, Olivier Dulaurent A, Bianchi D. *Langmuir*, **2001**,**17**(18):5496-5502

[34]Fanson P T, Delgass W N, Lauterbach J. *J. Catal.*, **2001**,**204**(1):35-52

[35]Avila M S, Vignatti C I, Apesteguía C R, et al. *Catal. Lett.*, **2010**,**134**(1/2):118-123